ORIGINAL RESEARCH

Diagnostic Accuracy of CT Angiography with Matched Mask Bone Elimination for Detection of Intracranial Aneurysms: Comparison with Digital Subtraction Angiography and 3D Rotational Angiography

M. Romijn
H.A.F. Gratama van Andel
M.A. van Walderveen
M.E. Sprengers
J.C. van Rijn
W.J. van Rooij
H.W. Venema
C.A. Grimbergen
G.J. den Heeten
C.B. Majoie

BACKGROUND AND PURPOSE: Our aim was to determine the diagnostic accuracy of multisection CT angiography combined with matched mask bone elimination (CTA-MMBE) for detection of intracranial aneurysms compared with digital subtraction angiography (DSA) and 3D rotational angiography (3DRA).

MATERIALS AND METHODS: Between January 2004 and February 2006, 108 patients who presented with clinically suspected subarachnoid hemorrhage underwent both CTA-MMBE and DSA for diagnosis of an intracranial aneurysm. Two neuroradiologists, independently, evaluated 27 predefined vessel locations in the CTA-MMBE images for the presence of an aneurysm. After consensus, diagnostic accuracy of CTA was calculated per predefined location and per patient. Interobserver agreement was calculated with κ statistics.

RESULTS: In 88 patients (81%), 117 aneurysms (82 ruptured, 35 unruptured) were present on DSA. CTA-MMBE detected all ruptured aneurysms except 1. Overall specificity, sensitivity, positive predictive value, and negative predictive value of CTA-MMBE were 0.99, 0.90, 0.98, and 0.95 per patient and 0.91, 1.00, 0.97, and 0.99 per location, respectively. Sensitivity was 0.99 for aneurysms $\geq$3 mm and 0.38 for aneurysms $<$3 mm. Interobserver agreement for aneurysm detection was excellent (κ value of 0.92 per location and 0.80 per patient).

CONCLUSION: CTA-MMBE is accurate in detecting intracranial aneurysms in any projection without overprojecting bone. CTA-MMBE has limited sensitivity in detecting very small aneurysms. Our data suggest that DSA and 3DRA can be limited to the vessel harboring the ruptured aneurysm before endovascular treatment, after detection of a ruptured aneurysm with CTA.

In current clinical practice, CT angiography (CTA) is the most frequently used noninvasive diagnostic tool for detection of intracranial aneurysms in the acute setting.[1-8] However, detection of intracranial aneurysms by CTA is limited because axial source section evaluation is tedious and 3D visualization is hampered by overprojecting bone, especially in the region of the skull base.[2,9-13] Several methods to remove bone, such as subtraction and manual or automated bone editing, have been developed.[7,8,14-19] Drawbacks of these methods are the complexity of use, dependence on the user, or high dose of radiation.

Matched mask bone elimination (MMBE) is a relatively new technique to remove bone from CTA source images (CTA-MMBE) in an automatic and user-independent way with little additional radiation dose.[20-22] In CTA-MMBE, a second nonenhanced low-dose scan (about a quarter of the radiation dose of a regular CTA) is used to identify bony structures that can subsequently be masked in the CTA scan.

Digital subtraction angiography (DSA) is the gold standard for detection of intracranial aneurysms. Extension of DSA with 3D rotational angiography (3DRA) can further improve detection of intracranial aneurysms that may be obscured by overprojecting vessels.[23-25] The advantages of DSA over CTA are superior spatial and contrast resolution, no interference of bony structures, and the possibility to perform direct endovascular interventions.[26,27] However, DSA is an invasive technique with a small but significant risk of neurologic complications, estimated to occur in 0.3%–1.8% of patients.[28,29]

The purpose of this study was to determine the diagnostic accuracy of CTA-MMBE for detection of intracranial aneurysms in a large patient population with clinically suspected subarachnoid hemorrhage (SAH) with DSA and 3DRA as reference standards.

Materials and Methods

Patients

Between January 2004 and February 2006, 108 patients who presented with clinically suspected SAH underwent both CTA-MMBE and DSA for diagnosis of an intracranial aneurysm. Of 108 patients, 102 had SAH confirmed by CT or lumbar puncture. There were 81 women and 27 men with a mean age of 56 years (median, 53 years; range, 19–92 years). In general, when 1 or more aneurysms were found on CTA or DSA, additional 3DRA was performed for pretreatment planning. Approval from the institutional review board for review of the patient's medical records and images was obtained. Because CTA-MMBE and DSA/3DRA were part of routine clinical practice, no approval was required to perform these imaging techniques in the patient group.

Received February 26, 2007; accepted after revision May 7.

From the Departments of Radiology (M.R., M.A.v.W., M.E.S., J.C.v.R., H.W.V., G.J.d.H., C.B.M.) and Medical Physics (H.A.F.G.v.A., H.W.V., C.A.G.), Academic Medical Center, University of Amsterdam, Amsterdam, the Netherlands; and the Department of Radiology (W.J.v.R.), St. Elisabeth Ziekenhuis, Tilburg, the Netherlands.

Please address correspondence to C.B. Majoie, MD, PhD, Department of Radiology, Room G1-223.2, Academic Medical Center, University of Amsterdam, Meibergdreef 9, 1105 AZ Amsterdam, the Netherlands; e-mail: c.b.majoie@amc.uva.nl

DOI 10.3174/ajnr.A0741

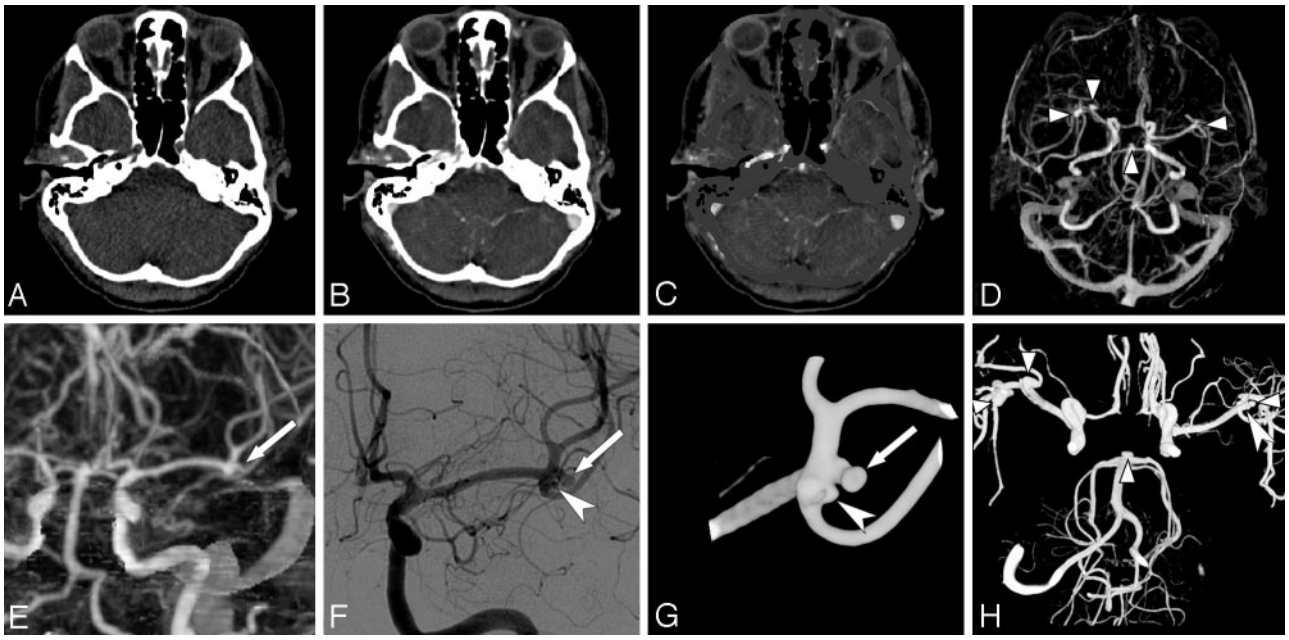

Fig 1. Illustration of a MMBE procedure in a 44-year-old woman with a ruptured right middle cerebral artery (MCA) aneurysm. *A–C,* Axial images of nonenhanced low-dose CT, CTA, and CTA after MMBE. *D,* Axial MIP obtained after MMBE shows 2 right MCA aneurysms, 1 left MCA aneurysm, and a basilar tip aneurysm (*arrowheads*). *E,* Coronal MIP image of the left MCA shows a 2.8-mm MCA aneurysm (*arrow*) and deceptive thickening of the MCA bifurcation. *F,* DSA shows the same aneurysm (*arrow*) as in *E,* with an additional 1.6-mm MCA aneurysm (*large arrowhead*). *G,* 3DRA more clearly shows both MCA aneurysms (*arrow* and *large arrowhead*). *H,* Composite image of three 3DRAs of both ICAs and the right vertebral artery shows all 5 aneurysms (*small arrowheads* and *large arrowhead*).

Imaging

Description of the technique of CTA-MMBE has been published previously.[20] Parameter settings were used as found optimal by van Straten et al.[22] Briefly, in MMBE, an additional nonenhanced low-dose spiral CT scan (65 mAs) was used to identify bony structures that were subsequently masked on CTA images (Fig 1*A–C*). These scans were made on a 4-section spiral CT scanner (MX8000; Philips Medical Systems, Best, the Netherlands or Sensation 4; Siemens Medical Solutions, Erlangen, Germany). We used the following parameters: 120 kV, 250 mAs, 4 × 1 mm detector collimation; pitch of 0.875, section thickness of 1.3 mm, increment of 0.5 mm, 150-mm FOV, 512 × 512 matrix, and reconstruction kernels B (Philips Medical Systems) and H30f (Siemens Medical Solutions). Eighty to 100 mL of nonionic contrast material was injected in a cubital vein at a rate of 4 mL/s. Scanning delay was automatically adjusted by a bolus-tracking technique.

CT and CTA images were sent to a workstation, and bone was removed automatically within 3 minutes by using the MMBE technique. CTA scans with masked bone were further processed in standardized maximum-intensity-projection (MIP) images: 40 images of different viewing angles rotated in a vertical and horizontal axis (Fig 1*D*).[8,30] After creation of a volume of interest, additional MIP images were made without venous structures.

DSA and 3DRA were performed by an experienced neuroradiologist on a single-plane angiographic unit (Integris Allura Neuro; Philips Medical Systems). Most angiograms were obtained with the patient under general anesthesia before coiling. Through a 6F catheter positioned in an internal carotid artery (ICA) or vertebral artery, 6- to 8-mL nonionic contrast was injected, and filming was performed in 2–3 projections at a frame rate of 2 per second. For 3DRA, 100 images were acquired during a 240° rotational run in 8 seconds with 15- to 21-mL contrast medium at 3 mL/s. On a dedicated workstation, 3D images were constructed and evaluated. Screen shots in multiple projections of volume-rendered 3D images were stored.

Image Evaluation

CTA-MMBE. For the purpose of this study, CTA source images and MIP images were anonymized and evaluated independently by 2 neuroradiologists blinded to clinical data and diagnostic CT and DSA results. CTA-MMBE image quality was rated as "good," "fair," "moderate," or "poor" and the extent of bone removal, as "complete," "near-complete," or "incomplete." "Near-complete" bone removal was defined as the presence of tiny bone remnants or small calcifications (Fig 2*A*, -*B*). Bone removal was "incomplete" when large bone remnants were present. Both readers recorded reasons for moderate or poor image quality. Twenty-seven predefined locations, subdivided into 4 subgroups, needed to be observed by each reader (Table 1). These 27 predefined locations were evaluated in all patients, resulting in the observation of 2916 locations in total. For interobserver discrepancies in detection of aneurysms, consensus was reached.

DSA and 3DRA. DSA images in combination with screen shots of 3DRA, if available, were used as reference standards.[26,27] Images were re-evaluated by an experienced interventional neuroradiologist. The observer needed to evaluate all visible locations from the 27 predefined locations, which depended on the number of vessels catheterized. Aneurysm size as measured on 3DRA was recorded. If 3DRA was not available, aneurysm size was estimated from comparison with the ICA (4 mm) or basilar artery (3 mm). Finally, rupture status of the aneurysm, derived from all image techniques, was assessed.

With DSA, 2188 of 2916 possible predefined aneurysm locations (75%) in 108 patients could be re-evaluated. 3DRA was available in 784 of 2188 locations (36%).

Statistical Analysis

The diagnostic accuracy of CTA-MMBE was calculated for 2188 locations observed with both DSA and CTA. Sensitivity, specificity, positive predictive value (PPV), negative predictive value (NPV), and exact 2-sided 95% confidence intervals (CI) were calculated for aneu-

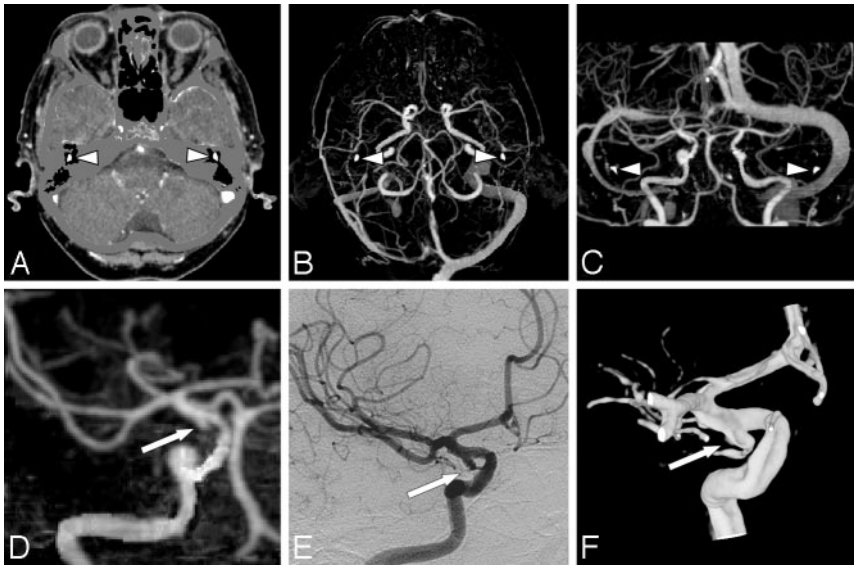

Fig 2. A 77-year-old woman with SAH and a false-positive-aneurysm finding on CTA. *A,* Axial CTA-MMBE image shows near complete bone removal as only the auditory ossicles (*arrowheads*) are not masked. *B* and *C,* Axial MIP and coronal MIP with small bone remnants of auditory ossicles (*arrowheads*), which do not hinder evaluation. *D,* Coronal MIP of a volume of interest with a small bulge of the right ICA interpreted as a small aneurysm (*arrow*). This infundibulum was mistaken for an aneurysm because the posterior communicating artery (PcomA) is not visible. *E* and *F,* DSA and 3DRA show the infundibulum of small PcomA (*arrow*).

Table 1: Number of detected aneurysms on DSA and 3DRA on 27 predefined aneurysm locations in 4 subgroups

Subgroup	Location*	No. of Aneurysms
Anterior cerebral artery	Anterior communicating artery	32
	Pericallosal artery	4
ICA	ICA tip	3
	ICA, other locations	8
	Posterior communicating artery	20
MCA	M1 segment	7
	M2 segment	3
	Bifurcation	21
Posterior circulation	Anterior inferior cerebellar artery	0
	Basilar tip	8
	Basilar trunk	2
	Posterior cerebral artery	1
	Posterior inferior cerebellar artery	4
	Superior cerebellar artery	3
	Vertebral artery	1
Total		117

* All locations were left and right, except for the anterior communicating artery, basilar trunk, and basilar tip, resulting in 27 predefined locations.

Table 2: Overall CTA image quality and quality of bone removal in 108 patients

Quality	Observer A	Observer B
Overall CTA		
Good	80	92
Fair	22	11
Moderate	4	4
Poor	2	1
CTA-MMBE		
Complete	3	5
Near-complete	98	101
Incomplete	7	2

rysm detection.[31] Diagnostic accuracy was also calculated per patient, per aneurysm size, per observed location, and per aneurysm location in 4 subgroups. Interobserver variability with percentages of agreement was calculated with κ statistics, with $\kappa \geq 0.80$ defined as excellent agreement; $\kappa = 0.60–0.79$, as good agreement; $\kappa = 0.40–0.59$, as moderate agreement; $\kappa = 0.20–0.39$, as fair agreement; and $\kappa = 0–0.19$, as slight agreement. The McNemar test was used to verify whether significant differences between observers and consensus of CTA-MMBE were present on aneurysm detection.

Results

DSA and 3DRA Evaluations

In 88 of 108 patients (81%), 117 aneurysms (82 ruptured, 35 unruptured) were detected on DSA and 3DRA. In 20 patients, no aneurysms were found. A single aneurysm was detected in 66 patients; 2 aneurysms, in 17 patients; 3 aneurysms, in 4 patients; and 5 aneurysms, in 1 patient. Aneurysm locations are listed in Table 1. Mean aneurysm size was 5.9 mm (median, 5 mm; range, 1–16 mm). Of 117 detected aneurysms, 16 were <3 mm, 50 were 3–5.9 mm, 36 were 6–10 mm, and 15 were >10 mm.

CTA Evaluations

Overall CTA-MMBE image quality and extent of bone removal evaluation for both observers are listed in Table 2. Reasons for poor or moderate image quality or incomplete bone removal (15 patients) were patient movement during scanning (8 patients) and insufficient arterial contrast combined with overprojecting venous structures (7 patients).

Overall diagnostic performance of CTA-MMBE for detection of intracranial aneurysms is listed in Table 3; diagnostic performance per aneurysm subgroup location, in Table 4; and diagnostic performance according to aneurysm size, in Table 5.

With CTA-MMBE, observer A detected 102 of 117 aneurysms (87%) (79 ruptured, 23 unruptured) and observer B, 103 (88%) (80 ruptured, 23 unruptured). After consensus, 11 aneurysms (9%) (1 ruptured, 10 unruptured) remained undetected. Observer A found 1 false-positive finding and observer B found 5 false-positive findings; after consensus, 3 false-positive findings remained. The false-positive finding of observer A proved to be cavernous sinus enhancement; the 5 false-positive findings of observer B were 3 infundibula (Fig 2*C*, -*D*), 1 ICA loop, and 1 local thickening of the pericallosal artery.

Table 3: Overall comparative diagnostic performance of CTA-MMBE*

	Sensitivity	Specificity	PPV	NPV
Per patient				
Observer A	0.94 (83/88)	0.95 (19/20)	0.99 (83/84)	0.79 (19/24)
95% CI	0.87–0.98	0.75–1.00	0.93–1.00	0.59–0.91
Observer B	0.99 (87/88)	0.90 (18/20)	0.98 (87/89)	0.95 (18/19)
95% CI	0.93–1.00	0.69–0.98	0.92–1.00	0.74–1.00
Consensus	0.99 (87/88)	0.90 (18/20)	0.98 (87/89)	0.95 (18/19)
95% CI	0.93–1.00	0.69–0.98	0.92–1.00	0.74–1.00
Per location				
Observer A	0.87 (102/117)	1.00 (2070/2071)	0.99 (102/103)	0.99 (2070/2085)
95% CI	0.80–0.92	1.00–1.00	0.94–1.00	0.99–1.00
Observer B	0.88 (103/117)	1.00 (2066/2071)	0.95 (103/108)	0.99 (2066/2080)
95% CI	0.81–0.93	0.99–1.00	0.89–0.98	0.99–1.00
Consensus	0.91 (106/117)	1.00 (2068/2071)	0.97 (106/109)	0.99 (2068/2079)
95% CI	0.84–0.95	1.00–1.00	0.92–0.99	0.99–1.00

* Numbers between parentheses are aneurysms or locations. With DSA, 117 aneurysms were detected in 88 patients on 2188 predefined observed locations.

Table 4: Diagnostic performance of CTA according to aneurysm location in subgroups*

Location	Sensitivity	Specificity	PPV	NPV
Anterior cerebral artery	0.97 (35/36)	1.00 (81/81)	1.00 (35/35)	0.99 (81/82)
95% CI	0.81–0.99	0.95–1.00	0.88–1.00	0.93–1.00
ICA	0.81 (25/31)	0.97 (83/86)	0.89 (25/28)	0.93 (83/89)
95% CI	0.63–0.91	0.90–0.99	0.72–0.97	0.86–0,97
MCA	0.90 (28/31)	1.00 (86/86)	1.00 (28/28)	0.97 (86/89)
95% CI	0.74–0.97	0.95–1.00	0.86–1.00	0.90–0.99
Posterior circulation	0.95 (18/19)	1.00 (98/98)	1.00 (18/18)	0.99 (98/99)
95% CI	0.74–1.00	0.95–1.00	0.79–1.00	0.94–1.00

* Numbers between parentheses are aneurysms.

Table 5: Diagnostic performance of CTA according to aneurysm size*

Size	Sensitivity	PPV
<3 mm	0.38 (6/16)	0.86 (6/7)
95% CI	0.18–0.61	0.57–0.99
3–5.9 mm	0.98 (49/50)	0.98 (49/50)
95% CI	0.89–1.00	0.89–1.00
6–10 mm	1.00 (36/36)	0.97 (36/37)
95% CI	0.89–1.00	0.85–1.00
>10 mm	1.00 (15/15)	1.00 (15/15)
95% CI	0.76–1.00	0.76–1.00

* Numbers between parentheses are aneurysms.

Sensitivity for detecting aneurysms ≥3 mm was 0.99, and for aneurysms <3 mm sensitivity was 0.38.

Characteristics of 11 aneurysms undetected after consensus with reasons for missing them are listed in Table 6. Ten of 11 missed aneurysms were ≤2.5 mm and were additional unruptured aneurysms in patients harboring multiple aneurysms (see example in Fig 1*D–H*). One missed aneurysm was a 4-mm ruptured dissecting posterior inferior cerebellar artery (PICA) aneurysm on a poor-quality CTA-MMBE due to patient movement. Another missed aneurysm was a 2.5-mm ophthalmic aneurysm in direct contact with the anterior clinoid process, which appeared smaller on MIP compared with the nonmasked CTA source images due to the applied MMBE technique and was, therefore, evaluated as an irregularity of the ICA. Most missed aneurysms were located on the ICA (5 of 11), and consequently, sensitivity for detection of aneurysms located on the ICA was significantly lower than that for other subgroup locations (Table 4).

Interobserver agreement per aneurysm location and per patient was excellent ($\kappa = 0.92$ with 99% agreement per location and $\kappa = 0.80$ with 94% agreement per patient, respectively). Due to the high number of negative aneurysm locations, observer agreement per patient was the most representative value. The McNemar test showed no significant differences between observers for aneurysm detection per patient and per location and for observers and consensus.

Discussion

In this study, we found high sensitivities and specificities of CTA-MMBE for detection of intracranial aneurysms with excellent interobserver agreement. Only 1 small dissecting aneurysm out of 82 ruptured aneurysms was not detected due to poor quality CTA-MMBE by patient movement. Other undetected aneurysms were very small unruptured aneurysms additional to a detected ruptured aneurysm. As in other studies, several shortcomings of CTA-MMBE and MIP images leading to misinterpretation were apparent, such as difficulties in differentiating arterial loops or infundibula from aneurysms (Fig 2*C*, *-D*), cavernous sinus contrast enhancement sometimes simulating or obscuring an aneurysm, and lack of depiction of very small aneurysms, especially located on the ICA.[9,10]

Our study design differs in some aspects from earlier published reports comparing CTA and DSA.[2,3,32-34] Because DSA and 3DRA do not necessarily include all vascular territories, analysis of results was performed per predefined anatomic aneurysm location and not per detected aneurysm. To minimize verification bias, we also included patients with no aneurysms found on DSA and CTA. To resemble clinical practice, we did not discard low-quality CTA studies. We used high-quality DSA and 3DRA as a reference standard (most angiograms were obtained in patients under general anesthesia), and con-

Table 6: Retrospective evaluation of 11 aneurysms not detected with CTA-MMBE*

Aneurysm Location	Size (mm)	Visible in Retrospect on CTA	Main Reason for Missing Aneurysm
Ophthalmic artery	2.5	Yes	Very small, in direct contact with bony structure (anterior clinoid process) and evaluated as irregularity of the ICA
ICA cavernous segment	2.0	Yes	Very small and poor quality of CTA
ICA supraclinoid segment	2.0	Yes	Very small and evaluated as part of multilobulated aneurysm
ICA tip	1.8	No	Very small and poor quality of CTA
ICA tip	2.2	Yes	Very small
MCA	1.5	No	Very small and presence of vasospasm
MCA	2.0	Yes	Very small and only visible on 1 MIP image
MCA	1.6	Yes	Very small and evaluated as thickening of MCA bifurcation
Pericallosal artery	2.0	Yes	Very small
PICA	4.0	Yes	Dissecting aneurysm, vasospasm, and incomplete bone removal due to patient movement
PcomA	2.0	No	Very small and low arterial contrast

* All except 1 were <3 mm. One 4-mm aneurysm was undetected due to poor-quality CTA-MMBE.

sequently, aneurysms as small as 1–2 mm were easily detected (Fig 1*G*). This standard may partly explain the relatively low sensitivity in this study for these very small intracranial aneurysms.

Because our study design differed in analysis and calculation methods, comparison with other studies is of limited value. For instance, in another study with a comparable number of patients, higher sensitivity for the detection of aneurysms was reported (0.95 versus 0.91), but small aneurysms located on the ICA were excluded.[4] In general, results of this study are in concordance with 2 meta-analyses.[26,27]

One could suspect that the relatively low sensitivity for small aneurysms could be attributed to the MMBE technique. However, of 11 missed aneurysms, only one 2.5-mm (ophthalmic) aneurysm was directly adjacent to a bony structure. This aneurysm appeared smaller on MIP compared with the nonmasked CTA source images due to the applied MMBE technique. All other missed aneurysms were not directly adjacent to bone, so MMBE could be excluded as a cause of missing them.

Our results and those of others suggest that complete DSA is no longer mandatory as a diagnostic tool in patients with good-quality CTA. Only in patients with confirmed SAH and poor-quality CTAs should complete diagnostic DSA be performed. Detection of a ruptured aneurysm with CTA can be followed by selective DSA of the vessel harboring the aneurysm before endovascular treatment, thereby reducing complication risk and procedural time. If this strategy were applied to the present study population, only very small additional unruptured aneurysms would go undetected. The rupture risk of very small additional aneurysms is extremely low.[35]

Because undetected small aneurysms may grow with time, however, a follow-up strategy in patients with coiled intracranial aneurysms should be DSA of the vessel harboring the aneurysm after 6 months and MRA at a later date, for example after 12–18 months and possibly yearly thereafter. With this strategy, growing initially undetected small aneurysms or de novo aneurysms will be detected in a timely manner. Patients with clipped aneurysms can be followed with CTA, especially when titanium clips were used.[36-38]

Manual bone editing in CTA is time-consuming (approximately 20 minutes) and user-dependent and requires knowledge of vascular anatomy.[8,18] In contrast, MMBE for bone removal is fully automatic and user-independent. MMBE removed bone adequately in all patients with good or fair quality CTA examinations with only insignificant small remnants of bone or calcifications (Fig 2 *A*, -*B*). When CTA examinations were of moderate or poor quality, CTA-MMBE and MIP images were also of lower quality. The main causes for reduced CTA image quality were patient movement during scanning, insufficient arterial contrast, and overprojection of veins. In case of patient movement during scanning, the incomplete bone removal was restricted to section positions at which movement occurred.

The question of whether MMBE has additional value in aneurysm detection remains unanswered in this study because we did not compare CTA-MMBE with a standard CTA technique. Subjectively however, MMBE offers easier and quicker viewing of reconstructed images without hindering bony structures. Average reading time per case was approximately 10 minutes, which is shorter than other CTA reading times reported (15–20 minutes).[39,40]

The use of 16- or 64-section CT scanners with shorter scanning times, thinner sections, and volume-rendered image display will improve the image quality of CTA. This may lead to higher sensitivity for detection of very small aneurysms and improved evaluation of aneurysm characteristics to assess the mode of treatment (surgical or endovascular).

Conclusion

CTA-MMBE is an accurate imaging technique for detection of intracranial aneurysms, allowing rapid aneurysm visualization on MIP images in any projection without overprojecting bone in a fully automatic and operator-independent way. CTA-MMBE has limited sensitivity in detecting aneurysms <3 mm with the use of 4-section CT scanners. Our data suggest that DSA and 3DRA can be limited to the vessel harboring the ruptured aneurysm before endovascular treatment, after detection of a ruptured aneurysm with CTA.

References

1. Kouskouras C, Charitanti A, Giavroglou C, et al. **Intracranial aneurysms: evaluation using CTA and MRA—correlation with DSA and intraoperative findings.** *Neuroradiology* 2004;46:842–50
2. Yoon DY, Lim KJ, Choi CS, et al. **Detection and characterization of intracra-**

nial aneurysms with 16-channel multidetector row CT angiography: a prospective comparison of volume-rendered images and digital subtraction angiography. *AJNR Am J Neuroradiol* 2007;28:60–67
3. Karamessini MT, Kagadis GC, Petsas T, et al. **CT angiography with three-dimensional techniques for the early diagnosis of intracranial aneurysms: comparison with intra-arterial DSA and the surgical findings.** *Eur J Radiol* 2004;49:212–23
4. Hoh BL, Cheung AC, Rabinov JD, et al. **Results of a prospective protocol of computed tomographic angiography in place of catheter angiography as the only diagnostic and pretreatment planning study for cerebral aneurysms by a combined neurovascular team.** *Neurosurgery* 2004;54:1329–40
5. Teksam M, McKinney A, Casey S, et al. **Multi-section CT angiography for detection of cerebral aneurysms.** *AJNR Am J Neuroradiol* 2004;25:1485–92
6. Matsumoto M, Sato M, Nakano M, et al. **Three-dimensional computerized tomography angiography-guided surgery of acutely ruptured cerebral aneurysms.** *J Neurosurg* 2001;94:718–27
7. Imakita S, Onishi Y, Hashimoto T, et al. **Subtraction CT angiography with controlled-orbit helical scanning for detection of intracranial aneurysms.** *AJNR Am J Neuroradiol* 1998;19:291–95
8. Velthuis BK, van Leeuwen MS, Witkamp TD, et al. **CT angiography: source images and postprocessing techniques in the detection of cerebral aneurysms.** *AJR Am J Roentgenol* 1997;169:1411–17
9. Fishman EK, Ney DR, Heath DG, et al. **Volume rendering versus maximum intensity projection in CT angiography: what works best, when, and why.** *Radiographics* 2006;26:905–22
10. Tomandl BF, Kostner NC, Schempershofe M, et al. **CT angiography of intracranial aneurysms: a focus on postprocessing.** *Radiographics* 2004;24:637–55
11. Jayaraman MV, Mayo-Smith WW, Tung GA, et al. **Detection of intracranial aneurysms: multi-detector row CT angiography compared with DSA.** *Radiology* 2004;230:510–18
12. Villablanca JP, Martin N, Jahan R, et al. **Volume-rendered helical computerized tomography angiography in the detection and characterization of intracranial aneurysms.** *J Neurosurg* 2000;93:254–64
13. Villablanca JP, Jahan R, Hooshi P, et al. **Detection and characterization of very small cerebral aneurysms by using 2D and 3D helical CT angiography.** *AJNR Am J Neuroradiol* 2002;23:1187–98
14. Fishman EK, Liang CC, Kuszyk BS, et al. **Automated bone editing algorithm for CT angiography: preliminary results.** *AJR Am J Roentgenol* 1996;166:669–72
15. Fiebich M, Straus CM, Sehgal V, et al. **Automatic bone segmentation technique for CT angiographic studies.** *J Comput Assist Tomogr* 1999;23:155–61
16. Casey SO, Alberico RA, Patel M, et al. **Cerebral CT venography.** *Radiology* 1996;198:163–70
17. Beier J, Oellinger H, Richter CS, et al. **Registered image subtraction for CT-, MR- and coronary angiography.** *Eur Radiol* 1997;7:82–89
18. Schwartz RB, Tice HM, Hooten SM, et al. **Evaluation of cerebral aneurysms with helical CT: correlation with conventional angiography and MR angiography.** *Radiology* 1994;192:717–22
19. Sakamoto S, Kiura Y, Shibukawa M, et al. **Subtracted 3D CT angiography for evaluation of internal carotid artery aneurysms: comparison with conventional digital subtraction angiography.** *AJNR Am J Neuroradiol* 2006;27:1332–37
20. Venema HW, Hulsmans FJ, den Heeten GJ. **CT angiography of the circle of Willis and intracranial internal carotid arteries: maximum intensity projection with matched mask bone elimination-feasibility study**. *Radiology* 2001;218:893–98
21. Majoie CB, van Straten M, Venema HW, et al. **Multisection CT venography of the dural sinuses and cerebral veins by using matched mask bone elimination.** *AJNR Am J Neuroradiol* 2004;25:787–91
22. van Straten M, Venema HW, Streekstra GJ, et al. **Removal of bone in CT angiography of the cervical arteries by piecewise matched mask bone elimination.** *Med Phys* 2004;31:2924–33
23. Anxionnat R, Bracard S, Ducrocq X, et al. **Intracranial aneurysms: clinical value of 3D digital subtraction angiography in the therapeutic decision and endovascular treatment.** *Radiology* 2001;218:799–808
24. Sugahara T, Korogi Y, Nakashima K, et al. **Comparison of 2D and 3D digital subtraction angiography in evaluation of intracranial aneurysms.** *AJNR Am J Neuroradiol* 2002;23:1545–52
25. Tanoue S, Kiyosue H, Kenai H, et al. **Three-dimensional reconstructed images after rotational angiography in the evaluation of intracranial aneurysms: surgical correlation.** *Neurosurgery* 2000;47:866–71
26. Chappell ET, Moure FC, Good MC. **Comparison of computed tomographic angiography with digital subtraction angiography in the diagnosis of cerebral aneurysms: a meta-analysis.** *Neurosurgery* 2003;52:624–31
27. White PM, Wardlaw JM, Easton V. **Can noninvasive imaging accurately depict intracranial aneurysms? A systematic review.** *Radiology* 2000;217:361–70
28. Willinsky RA, Taylor SM, TerBrugge K, et al. **Neurologic complications of cerebral angiography: prospective analysis of 2,899 procedures and review of the literature.** *Radiology* 2003;227:522–28
29. Cloft HJ, Joseph GJ, Dion JE. **Risk of cerebral angiography in patients with subarachnoid hemorrhage, cerebral aneurysm, and arteriovenous malformation: a meta-analysis.** *Stroke* 1999;30:317–20
30. Napel S, Marks MP, Rubin GD, et al. **CT angiography with spiral CT and maximum intensity projection.** *Radiology* 1992;185:607–10
31. Agresti A, Coull BA. **Approximate is better than "exact" for interval estimation of binomial proportions.** *Am Stat* 1998;52:119–26
32. Villablanca JP, Achiriolaie A, Hooshi P, et al. **Aneurysms of the posterior circulation: detection and treatment planning using volume-rendered three-dimensional helical computerized tomography angiography.** *J Neurosurg* 2005;103:1018–29
33. Chen CY, Hsieh SC, Choi WM, et al. **Computed tomography angiography in detection and characterization of ruptured anterior cerebral artery aneurysms at uncommon location for emergent surgical clipping.** *Clin Imaging* 2006;30:87–93
34. Korogi Y, Takahashi M, Katada K, et al. **Intracranial aneurysms: detection with three-dimensional CT angiography with volume rendering–comparison with conventional angiographic and surgical findings.** *Radiology* 1999;211:497–506
35. Wermer MJ, van der Schaaf IC, Algra A, et al. **Risk of rupture of unruptured intracranial aneurysms in relation to patient and aneurysm characteristics: an updated meta-analysis.** *Stroke* 2007;38:1404–10. Epub 2007 Mar 1
36. Sakuma I, Tomura N, Kinouchi H, et al. **Postoperative three-dimensional CT angiography after cerebral aneurysm clipping with titanium clips: detection with single detector CT—comparison with intra-arterial digital subtraction angiography**. *Clin Radiol* 2006;61:505–12
37. Steiger HJ, van Loon JJ. **Virtues and drawbacks of titanium alloy aneurysm clips**. *Acta Neurochir Suppl* 1999;72:81–88
38. van der Schaaf I, Velthuis BK, Wermer MJ, et al. **Multislice computed tomography angiography screening for new aneurysms in patients with previously clip-treated intracranial aneurysms: feasibility, positive predictive value, and interobserver agreement**. *J Neurosurg* 2006;105:682–88
39. El Khaldi M, Pernter P, Ferro F, et al. **Detection of cerebral aneurysms in nontraumatic subarachnoid haemorrhage: role of multislice CT angiography in 130 consecutive patients** [in English, Italian]. *Radiol Med (Torino)* 2007;112:123–37
40. Wintermark M, Uske A, Chalaron M, et al. **Multislice computerized tomography angiography in the evaluation of intracranial aneurysms: a comparison with intraarterial digital subtraction angiography**. *J Neurosurg* 2003;98:828–36